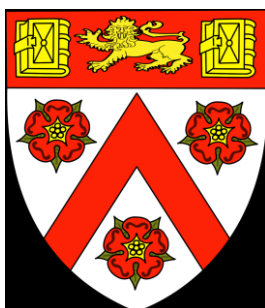


Fabrication and Characterization of Titanium-doped Hydroxyapatite Thin Films



Amit Y. Desai
Trinity College
University of Cambridge



Device Materials Group &
Cambridge Centre for Medical Materials
Department of Materials Science & Metallurgy

August 2007

This dissertation is submitted for the degree of
Master of Philosophy in Physics at the University of Cambridge

Declaration

I hereby declare that this dissertation is the result of my own work and includes nothing which is the outcome of work done in collaboration except where is specifically indicated in the text and bibliography and that my thesis is not substantially the same as any that I have submitted for a degree of diploma or other qualification at any other University. In addition, this dissertation falls within the word limit of 15,000 words, exclusive of tables, footnotes, bibliography, and appendices, as set by the Physics and Chemistry Degree Committee.

Amit Yogesh Desai

Abstract

Hydroxyapatite [$\text{Ca}_{10}(\text{PO}_4)_6(\text{OH})_2$, HA] is used in many biomedical applications including bone grafts and joint replacements. Due to its structural and chemical similarities to human bone mineral, HA promotes growth of bone tissue directly on its surface. Substitution of other elements has shown the potential to improve the bioactivity of HA. Magnetron co-sputtering is a physical vapour deposition technique which can be used to create thin coatings with controlled levels of a substituting element. Thin films of titanium-doped hydroxyapatite (HA-Ti) have been deposited onto silicon substrates at three different compositions.

With direct current (dc) power to the Ti target of 5, 10, and 15W films with compositions of 0.7, 1.7 and 2.0 at.% titanium were achieved. As-deposited films, 1.2 μm thick, were amorphous but transformed into a crystalline film after heat-treatment at 700°C. Raman spectra of the PO_4 band suggests the titanium does not substitute for phosphorous. X-ray diffraction revealed the c lattice parameter increases with additional titanium content. XRD traces also showed titanium may be phase separating into TiO_2 , a result which is supported by analysis of the Oxygen 1s XPS spectrum.

In-vitro observations show good adhesion and proliferation of human osteoblast (HOB) cells on the surface of HA-Ti coatings. Electron microscopy shows many processes (i.e. filopodia) extended from cells after day one *in-vitro* and a confluent, multi-layer of HOB cells after day three. These finding indicate that there may be potential for HA-Ti films as a novel implant coating to improve upon the bioactivity of existing coatings.

Acknowledgements

Having arrived in Cambridge at the start of October 2006, I was privileged to have the guidance and support of my two supervisors: Dr. Zoe H. Barber and Dr. Serena M. Best. Zoe and Serena helped me organize my research goals to fit within my limited time in Cambridge while also supporting my extra-curricular activities. They both remained positive in light of changes midway through my work and encouraged me to present my work within the university and at a conference.

My colleagues in both the Device Materials Group as well as the Cambridge Centre for Medical Materials have provided a fun, light-hearted environment in which to carry out my work. A special thanks goes to Mr. Junyi Ma whose extensive work on developing a pristine sputtering target allowed me to conduct my experiments with confidence.

Individual thanks go to the following groups for their assistance with obtaining experimental results: Device Materials Group (Dr. Nadia Stelmashenko), CCMM (Mr. Wayne Hough), Electron Microscopy Group (Mr. David J. Vowles and Mr. David A. Nicol), Macromolecular Materials Laboratory (Mr. Robert Cornell, Dr. Krzysztof Koziol), Orthopaedic Research Unit (Dr. Roger A. Brooks), and X-ray Facilities (Ms. Mary E. Vickers and Mr. Andrew J. Moss), Department of Chemistry and Materials at Manchester Metropolitan University (Dr. Vlad M. Vishnyakov), Department of Physiology, Development and Neuroscience (Dr. Jeremy Skepper).

I was able to fund my studies in Cambridge thanks to a National Science Foundation (USA) Graduate Research Fellowship. I am also grateful to Trinity College for complementing my research by providing a vibrant social atmosphere.

Finally, I thank my parents for their unwavering support of my academic journey, regardless of where it takes me.

Table of Contents

	Page
Declaration	i
Abstract	ii
Acknowledgements	iii
Table of Contents	iv
List of Figures	vi
List of Tables	viii
Chapter 1 Introduction	
1.1 Background	1
1.2 Objectives	2
1.3 Scope	3
Chapter 2 Calcium Phosphates as Coatings	
2.1 Calcium Phosphates	4
2.2 Hydroxyapatite	5
2.2.1 Use of HA as an Implant Coating	6
2.2.2 Substituted Hydroxyapatite	7
2.2.2.1 Carbonate	7
2.2.2.2 Magnesium	8
2.2.2.3 Silicon	9
2.2.2.4 Titanium	10
2.3 Studying the Bioactivity of Coatings	11
Chapter 3 Review of CaP Coating Production Methods	
3.1 Introduction	14
3.2 Plasma Spraying	15
3.3 Sol-gel and Biomimetic Processes	16
3.4 Principles of Magnetron Sputtering	18
3.5 Physicochemical Properties of Sputtered Coatings	20
3.5.1 Heat treatment of Sputtered Coatings	21
3.5.2 <i>In-vivo</i> Study of Sputtered Coatings	21
3.5.3 Sputtering of Doped-Hydroxyapatite Thin Films	22
3.6 Summary	23
Chapter 4 Experimental Methods for Film Fabrication	
4.1 Substrates & Targets	24
4.2 Magnetron Co-sputtering	24
4.3 Heat Treatment	27

Chapter 5	Characterization of Thin Films	
5.1	Thickness and Composition.	28
5.1.1	Profilometry	28
5.1.2	Energy Dispersive X-ray Spectroscopy	28
5.1.3	Results	29
5.2	Surface Morphology	30
5.2.1	Optical Microscopy	30
5.3	Crystal Structure and Unit-cell Parameters	31
5.3.1	X-Ray Diffraction	31
5.3.2	XRD Results	33
5.4	Surface Chemistry of HA-Ti Films	36
5.4.1	X-ray Photoelectron Spectroscopy (XPS)	36
5.4.2	XPS Results	36
5.5	Molecular Structure of HA-Ti Films	42
5.5.1	Raman Spectroscopy	42
5.5.2	Preliminary Results	43
Chapter 6	<i>In-Vitro</i> Observations	
6.1	Sample Preparation	45
6.2	Cell Cultures, Seeding, and Attachment	46
6.3	Electron Micrographs of Cells	47
6.4	Electron Micrographs of Coating Morphology	53
Chapter 7	Discussion	
7.1	Film Preparation	55
7.2	Substitution vs. Phase Separation	55
7.3	Additional Analysis	57
7.4	<i>In-Vitro</i> Observations	58
Chapter 8	Conclusions	60
Chapter 9	Future Work	61
References		62

List of Figures

	Page
Figure 2.1 Schematic representation of hydroxyapatite crystal structure.	6
Figure 2.2 Changes in lattice parameter with respect to increasing carbonate substitution.	8
Figure 2.3 Precipitated Ca-P on the surface of bioactive HA: (a) Needle-like Ca-P precipitates form as the HA granule undergoes dissolution. The HA has been dispersed in simulated body fluid for 1 day. (b) HA which was placed <i>in-vivo</i> for 12 weeks promotes the formation of bone apatite around the implant interface without dissolving.	12
Figure 2.4 Cellular response to bioinert versus bioactive materials: (a) MG-63 cell retains spherical morphology and has not spread on the bare titanium substrate; (b) MG-63 cells have attached and proliferated on the bioactive surface. Filopodia extend from the base of the cells as they spread.	13
Figure 3.1 Hip-replacement prosthesis 8 years after surgery (left) and original HA-coated titanium prosthetic (right).	14
Figure 3.2 Schematic of plasma spraying process. HA powder is fed into the plasma flame. The particles arrive with both high velocity and temperature at the substrate where they stack upon one another to build up the coating.	15
Figure 3.3 Schematic diagram illustrating magnetron sputtering system.	19
Figure 4.1 (a) Schematic diagram of co-sputtering system, (b) schematic of rotatable shield/mask.	26
Figure 5.1 Regions of continuous film after the onset of cracking due to heat-treatment (700°C in Ar-H ₂ O for 4 hours) in a representative sample.	30
Figure 5.2 XRD peaks for hydroxyapatite (ICDD 09-0432).	32
Figure 5.3 XRD Patterns for HA-Ti films: (a) as-deposited x-ray amorphous film, (b) example of sputtered HA thin-film heated at 700°C for 4 hrs.	33
Figure 5.4 XRD traces for HA-Ti films heat-treated to 700 °C in Ar-H ₂ O atmosphere for 4hrs: (a) 0.7 at. % Ti-HA, (b) 1.7 at. % Ti-HA, (c) 2.0 at. % Ti-HA.	34
Figure 5.5 Increasing <i>c</i> -axis lattice parameter with increasing titanium content.	35
Figure 5.6a Binding energy (eV) of carbon 1s.	37
Figure 5.6b Binding energy (eV) of oxygen 1s.	38

Figure 5.6c	Binding energy (eV) of phosphorous 2p. The red line represents the baseline.	38
Figure 5.6d	Binding energy (eV) of calcium 2p.	39
Figure 5.6e	XPS spectrum of carbon 1s signal before and after argon ion bombardment.	41
Figure 5.7	Raman spectra showing various Raman shifts for HA-Ti films: (a) Sample A3, heat-treated in argon only, (b) Sample B3, heat-treated in argon-water vapour.	43
Figure 5.8	Raman spectra of the PO ₄ (ν_1) absorption band for HA-Ti thin films (Ti-content 0.7, 1.7, 2.0 at. % annealed at 700C for 4hrs in Ar-H ₂ O).	44
Figure 6.1	Filopodia extend from an HOB cell on sample A1 (heat-treated at 700°C in Ar + H ₂ O; 2.0 at. % titanium doped hydroxyapatite).	47
Figure 6.2	A confluent layer of HOB cells forms on sample A1 (heat-treated at 700°C in Ar + H ₂ O; 2.0 at. % titanium doped hydroxyapatite) where cells were seeded at a higher density.	48
Figure 6.3	HOB cells attach and proliferate on sample A2 (as-sputtered thin film, 0.7 at.% HA-Ti) after one day.	49
Figure 6.4	Some HOB cells on sample A3 (Si substrate) retain a rounded morphology.	50
Figure 6.5	An HOB cell on sample A3 (Si substrate) shows extended filopodia and many processes on the cell surface.	50
Figure 6.6	A confluent layer of HOB cells on sample B1 (heat-treated at 700°C in Ar; 1.7 at.% HA-Ti) after three days <i>in-vitro</i> .	51
Figure 6.7	Many filopodia continue to extend from HOB cells on sample B1 after three days <i>in-vitro</i> . Cells have proliferated very well with some overlap.	52
Figure 6.8	A HOB cell appears to be dividing. Many surface processes indicate continued cell activity. Filopodia continue to extend from the well spread HOB cells on sample B1.	52
Figure 6.9	Cracking due to heat treatment on sample B1, after three days <i>in-vitro</i> .	53
Figure 6.10	Surface morphology of an as-sputtered sample (A3) <i>in-vitro</i> for 1 day. Higher magnification inset illustrates the difference in morphology when compared to heat-treated samples.	54

List of Tables

	Page
Table 2.1 Examples of CaP phases for biomedical applications.	4
Table 2.2 Chemical and structural comparison of teeth, bone, and HA.	5
Table 4.1 Crystallization atmosphere and sputtering conditions for HA-Ti films.	27
Table 5.1 DC input power (Ti target) vs. titanium content.	29
Table 5.2 Peak positions from XPS spectra of HA-Ti thin film.	40
Table 6.1 Samples used to collect electron micrographs (Section 6.3).	45

Chapter 1

Introduction

1.1 Background

The desire to introduce man-made materials into the treatment of the human body has prompted a wave of research into the field of biomaterials. An ever-present challenge in the area of biomaterials is to enhance the interface between biomaterial implants and the living tissue surrounding them. Some researchers in the field of orthopaedic biomaterials direct their focus on the fabrication and enhancement of bioactive properties of calcium-phosphates and in particular much interest has been directed towards the use of hydroxyapatite (HA).

Calcium phosphate biomaterials are frequently used in the repair of the dental and musculoskeletal systems. In the case of the dental system HA has been used as a coating for tooth-root implants. In the musculoskeletal systems, calcium phosphates play a variety of roles from spinal fusions to the replacement of major load-bearing joints.

Extended life-expectancies combined with increasingly active lifestyles have led to many bone-related ailments including increased susceptibility to bone fracture or excessive wearing of joints. As a result joint replacement surgeries have become omnipresent as a safe and effective way to improve the quality of life for patients suffering from joint ailments. One such type of joint replacement surgery is the total-hip arthroplasty (hip-replacement) which requires a metal stem (often titanium) to be fixed within the femur. The stem must be a strong material capable of bearing load and also integrating well with the surrounding bone tissue. Titanium implants themselves are harmless to the body, but do little to aid bone integration with the stem. One route to overcome this problem is to coat the implant with a material, such as HA, which mimics bone mineral thereby allowing the surrounding tissue to bond to the implant.

A common commercial method for coating metal implants for use with bone is plasma-spraying. While this technique is successful, it possesses a few drawbacks including the potential for the coating to delaminate. One alternative to plasma-spraying is sputtering, a physical vapour deposition technique, which yields excellent adhesion and uniform coverage to substrate materials. Sputtering also provides a simple method for doping calcium

phosphates with other ions at varying concentrations, an attractive option when designing substituted-HA.

Substitutions to HA have been shown to improve osteoconductivity, thereby promoting better attachment and proliferation of bone-forming cells. In the 1970's Carlisle *et. al.* showed that a Si-deficient diet led to poor bone mineralization and feather development in chickens.

Researchers have since attempted to add silicon to HA to enhance its biological response and this choice of substitution has shown positive results (Thian *et al.* 2006, Gibson *et. al* 1999). Although the specific mechanism through which substitutions in HA enhance its bioactivity have yet to be fully understood, there are many other dopants which may prove beneficial to HA. One such substitution which has yet to be explored in great detail is that of titanium into HA. Some researchers are presently investigating ways to develop TiO₂/HA hybrid coating due to the bioactive properties of both components. Such composites can be achieved by co-sputtering titanium and HA onto a substrate.

The successes that HA and TiO₂ have shown in promoting growth and proliferation of bone tissue both separately and in combination with one another give way to the objective of this research. A new technique will be employed to combine HA and Ti to investigate the potential for producing titanium-doped HA coatings and determining their biological cell response.

1.2 Objectives

This research aims to complete the following tasks;

1. Develop titanium-doped hydroxyapatite (HA-Ti) thin films by magnetron co-sputtering.
2. Investigate the effects of titanium doping on the crystal structure and surface chemistry of HA-Ti films.
3. Observe the biological response to HA-Ti films *in-vitro* using human osteoblast-like cells.

1.3 Outline

Chapter 1 of the thesis provides an overview and touches on the motivations behind this research. Chapter 2 provides an introduction to calcium-phosphates, in particular hydroxyapatite and its uses as an implant coating. Chapter 3 presents a survey of three methods used for making implant coatings with a focus on magnetron sputtering. Chapters 4 to 6 present and discuss the experimental results obtained. Chapter 7 provides a linked discussion of all results. Chapters 8 and 9 present the conclusions and future work.

The experimental section of this research is divided into three chapters. Chapter 4 provides a brief summary of the titanium-doped hydroxyapatite thin films produced by magnetron co-sputtering. Chapter 5 is divided into sections corresponding to each characterization technique applied to samples: profilometry, energy dispersive x-ray spectroscopy, microscopy, x-ray diffraction, x-ray photoelectron spectroscopy, and Raman spectroscopy. Chapter 6 presents *in-vitro* observations of cell response to the HA-Ti thin films.

Chapter 2

Calcium Phosphates as Coatings

2.1 Calcium Phosphates

Calcium phosphates (CaP) have been used for over 30 years in clinical applications (Shi 2006). There are a variety of compounds in the CaP family, many of which are used in biomedical applications. The stability of CaP compounds is controlled by the ratio of calcium to phosphorous, the amount of water present, the temperature at which they are processed as well as the pH of the surrounding environment. The table below (Table 2.1) outlines a few CaP phases along with their chemical formula and Ca/P ratio (Fernandez 1999).

Table 2.1 Examples of CaP phases for biomedical applications.

Phase	Formula	Ca/P ratio
Amorphous calcium phosphate (ACP)	n/a	n/a
Octacalcium phosphate (OCP)	$\text{Ca}_8(\text{HPO}_4)_2(\text{PO}_4)_4 \cdot 5\text{H}_2\text{O}$	1.33
Tricalcium phosphate (α or β TCP)	$\text{Ca}_3(\text{PO}_4)_2$	1.5
Hydroxyapatite (HA)	$\text{Ca}_2(\text{PO}_4)_6(\text{OH})_2$	1.67

Octacalcium phosphate is thought to be a biological precursor to apatite formation in bone and teeth (Brown 1962). OCP has been shown to convert to an apatite structure both *in-vivo* and *in-vitro*. A recent study demonstrated the important role of OCP in bone mineralization by showing improved bone formation on implanted OCP as compared to a hydrolyzed Ca-deficient HA with respect to filling bone defects (Suzuki 2006).

TCP is sometimes referred to by its chemical name calcium orthophosphate tribasic and exists as one of four polymorphs (α , β , γ , and super- α) (Gibson *et al* 1996). The γ polymorph is a high-pressure phase while super- α phase is observed at high temperatures (above 1500°C). Therefore it is mainly the α and β phases that are of interest as biomaterials. α - and β -TCP find application primarily in temporary scaffolds and in calcium phosphate bone cements. Bone cements, in general, are of interest because they are injectable, they can fill voids, and may serve as a resorbable scaffold material (Roemhildt 2006, Song 2007). It is also known that the dissolution of TCP is dependent upon its phase. In order of decreasing solubility α -TCP > β -TCP >> HA (Lin *et al.* 2001) which means under physiological conditions, HA is the most stable of the three materials.

Amorphous calcium phosphate is the least stable of the CaP phases in solution. It is typically the first phase formed during most rapid precipitation methods of forming CaP. ACP has been used in bone-cement (Takagi *et al.* 1998) as well as dental fillings (Dorozhkin 2007). Amorphous calcium phosphates have been used to develop mineral-releasing dental composites (Skrtic *et al.* 2004) as well as bone-implants for non-load bearing applications (Tadic *et al.* 2002).

2.2 Hydroxyapatite

Synthetic hydroxyapatite is similar in composition to the mineral component of bone and teeth. This similarity has led to interest in the development of HA materials for biomedical applications. The table below (Dorozhkin 2007) illustrates the chemical and structural similarities between HA, enamel, dentin, and bone.

Table 2.2 Chemical and structural comparison of teeth, bone, and HA.

Composition, wt%	Enamel	Dentin	Bone	HA
Calcium	36.5	35.1	34.8	39.6
Phosphorous	17.1	16.9	15.2	18.5
Ca/P ratio	1.63	1.61	1.71	1.67
Total inorganic (%)	97	70	65	100
Total organic (%)	1.5	20	25	--
Water (%)	1.5	10	10	--
Crystallographic properties: Lattice parameters ($\pm 0.003 \text{ \AA}$)				
<i>a</i> -axis (\AA)	9.441	9.421	9.41	9.430
<i>c</i> -axis (\AA)	6.880	6.887	6.89	6.891
Crystallinity index, (HA=100)	70-75	33-37	33-37	100

Crystallographically, hydroxyapatite belongs to the hexagonal system with the $P6_3/m$ space group. The 'P' indicates that HA is a primitive hexagonal system where $a = b \neq c$, $\alpha = \beta = 90^\circ$ and $\gamma = 60^\circ$ (Kay *et al.* 1964). A schematic representation of the crystal structure is provided in Figure 2.1 (Shi 2006).

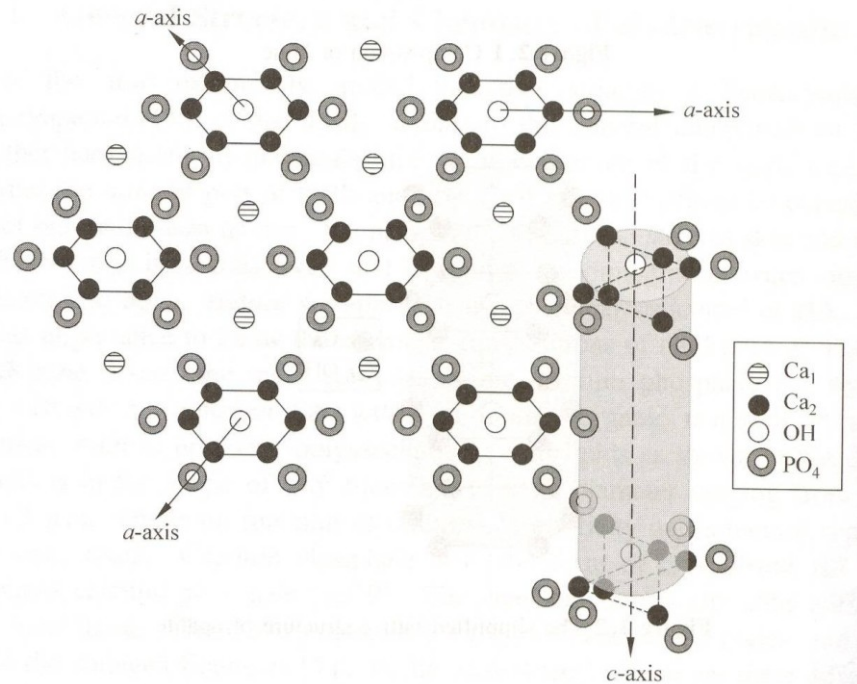


Figure 2.1 Schematic representation of hydroxyapatite crystal structure.

2.2.1 Use of HA as an Implant Coating

Hydroxyapatite is known to be bioactive, meaning bone growth is supported directly on the material's surface when placed next to bone. This response of hydroxyapatite sets it apart from the other CaP phases and has led to routine use in orthopaedic surgery in both powder and bulk form (Shi 2006). Wong *et al.* (1995) compared the osseointegration of commercial implants in the trabecular bone of mature miniature pigs for 12 weeks. Their results showed excellent osseointegration of the HA coated implant. More recent studies (Cao *et al.* 2006, Froimson *et al.* 2007) have also shown the successful osseointegration of HA coatings with surrounding bone tissue after an HA coated implant was placed within living bone. Cao *et al.* produced HA coated carbon/carbon (carbon-fiber reinforced carbon) composites, an alternative to the traditional metal stem used in total-hip arthroplasties, and placed these implants into the tibia of rabbits. Froimson *et al.* recently concluded that plasma-sprayed HA coated titanium implants showed excellent osseointegration during 10-year follow ups of 147 consecutive primary hip arthroplasties performed in 133 patients by a single surgeon during a 2-year interval.

While HA has demonstrated its ability to integrate with bone tissue it does not possess ideal mechanical properties to serve as a major load-bearing implant. Many orthopaedic implants are based on the use of metallic alloys such as stainless steel or titanium alloy. Metals,

however, do not form a direct bond with bone. Therefore there is interest in applying bioactive coatings to metal implants.

2.2.2 Substituted Hydroxyapatite

HA and bone mineral are somewhat different in composition and degree of crystallinity. Bone mineral is typically calcium deficient and contains carbonate substitutions. Other ions present in bone mineral include magnesium (Mg^{2+}), sodium (Na^+), potassium (K^+), fluoride (F^-), and chloride (Cl^-) ions. It has been proposed that the more appropriate chemical formula for biological HA is $(Ca, M)_{10}(PO_4, Y)_6(OH, X)_2$ where M represents a substitution cation and X and Y represent substitution anions (Shi 2006). These substitutions may cause changes in properties such as crystallinity, solubility, and ultimately biological response. It is these changes in HA which have led researchers to enhance the biological response of HA through substitution.

2.2.2.1 Carbonate

Carbonate-substituted hydroxyapatite is believed to be more similar to bone mineral than pure HA and serves to decrease the crystallinity of the apatite while increasing its rate of dissolution. The mechanism for the substitution of the carbonate (CO_3^{2-}) ion into the HA lattice is well defined (Driessens 1983). There exist two types of carbonate substitutions, referred to as Type *A* and Type *B* substitutions. Type *A* substitution takes place when the carbonate ion replaces the hydroxyl (OH^-) group whereas type *B* substitution takes place when the phosphate (PO_4^{3-}) group is replaced. Type *A* may be achieved by heat-treating HA in a carbon dioxide atmosphere whereas Type *B* may be formed by wet precipitation (Barralet *et al.* 1998) although it is more likely that both Type *A* and *B* substitutions occur.

The two carbonate substitutions have opposite effects on the HA lattice parameter. During type *A* substitution the larger carbonate group sits on the smaller hydroxyl site, expanding the *a*-axis and contracting the *c*-axis (Romo 1954). During type *B* substitution the smaller carbonate group sits on the larger phosphate site, contracting the *a*-axis while expanding the *c*-axis. Figure 2.2 illustrates these changes (Shi 2006).

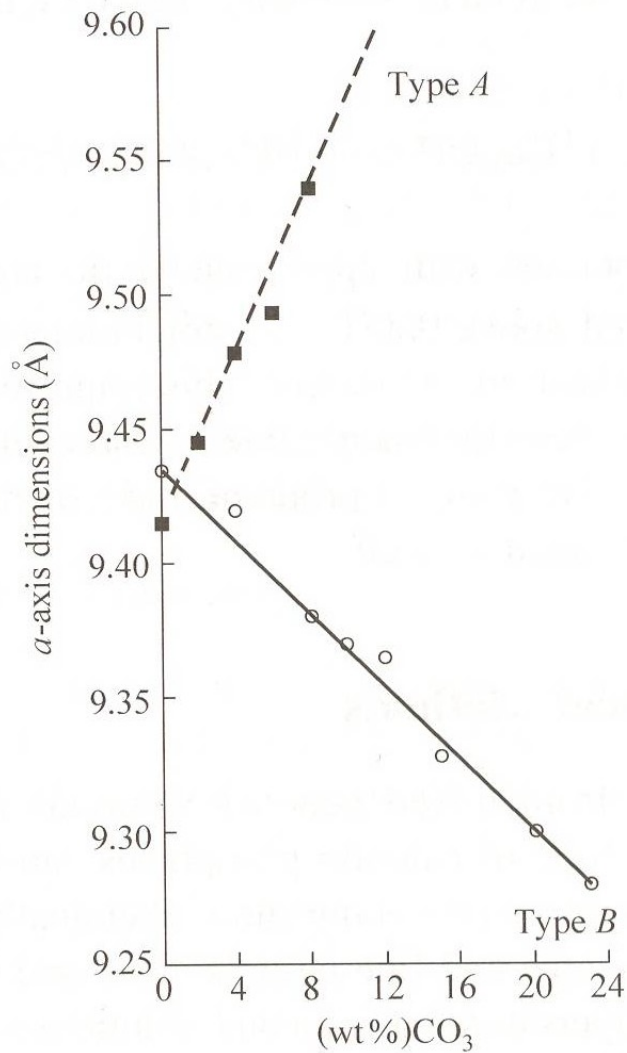


Figure 2.2 Changes in lattice parameter with respect to increasing carbonate substitution.

Researchers have proposed models for a type *AB* substitution in which the *a*-axis lattice parameter contracts while the *c*-axis lattice parameter expands (Barralet *et al.* 1998, Fleet and Liu 2007).

2.2.2.2 Magnesium

The importance of ions such as magnesium, zinc, copper, iron, and fluoride for normal bone metabolism have been documented. With approximately 25 grams of Mg in the body, its role is small, but vital. Magnesium is believed to be integral for bone formation and resorption via reactions at the surface of bone mineral (Ilich *et al.* 2000). Kakei *et al.* (1997) also demonstrated the importance of Mg in early-stage bone development through *in-vivo* tests.

A study by Landi *et al.* (2006) showed improved response of mesenchymal stem cells and MG-63 osteoblast-like cells with respect to adhesion, proliferation and metabolic activation

on 1 wt. % Mg–HA. More recently, Landi *et al.* (2007) have demonstrated biocompatible Mg substituted HA at 5.7 mol. % Mg. Serre *et al.* (1998) presented some interesting findings when introducing Mg into hydroxyapatite. Results showed that high magnesium content (20 wt.%) was cytotoxic to cell cultures during *in-vitro* testing and also suppressed the formation of a calcifying matrix around the cells.

The substitution of Mg into CaP phases has also shown that the magnesium helps to stabilize the beta-tricalcium phosphate phase (Gibson *et al.* 2002, Kannan *et al.* 2007). These findings are useful for those developing Ca-P bone cements. Mg substitution into CaP phases remains an active area of research.

2.2.2.3 Silicon

In the 1970's and 80's. Carlisle (1972, 1973, 1980) presented evidence that bone development was significantly hampered in chicks which were fed a silicon deficient diet. These findings were complemented by work which identified the presence of silicon in the bones of developing chicks and mice (Carlisle 1970, Landis *et al.* 1986). Since the initial finding regarding the role of silicon in bone development, efforts have been made to develop silicon-substituted hydroxyapatite. It is accepted that the silicon substitutes for the phosphorous in the HA unit cell as determined through FTIR studies of the absorption bands associated with the phosphate group (Gibson *et al.* 1999).

Both *in-vivo* and *in-vitro* testing has been performed. In a study using a rabbit model the addition of 0.8 wt. % silicon to hydroxyapatite has shown improved bone ingrowth ($37.5\% \pm 5.9$) compared to undoped HA ($22.0\% \pm 6.5$), as well as better bone/implant coverage ($59.8\% \pm 7.3$) compared to HA ($47.1\% \pm 3.6$) (Patel *et al.* 2002). In addition to better coverage, the rate at which bone-cells adhere and proliferate on SiHA coatings has been investigated *in-vitro* using human osteoblast-like cells (Thian *et al.* 2007). Results from Thian *et al.* show greater metabolic activity between days 2 and 4 on SiHA (up to 4.9 wt.% Si) samples as compared to undoped HA.

Porter *et al.* (2003) investigated the dissolution of SiHA and observed the following trend with respect to rate of dissolution: 1.5 wt% Si-HA > 0.8 wt% Si-HA > undoped HA. It was reported that this trend is related to the quantity of triple junctions and grain boundaries present as a result of increased substitution.

2.2.2.4 Titanium

TiO₂ forms naturally as the native oxide layer on titanium alloys which are implanted into the body. This oxide layer serves to control the release of ions from the metal alloy, which in large quantities can be toxic to the human body. Kitsugi *et al* (1996) performed an *in-vivo* study using a rabbit model and observed improved bone-bonding ability of titanium implants when coated with TiO₂. A study (Wen *et al.* 1998) later proposed that the attraction of OH⁻ groups to TiO₂ in aqueous solution plays a role in precipitation of CaP minerals. Li *et al.* (1996) also demonstrated the excellent bioactivity of TiO₂ both *in-vitro* and *in-vivo* using sol-gel coatings.

The introduction of titanium into HA has not yet been approached from the perspective of a cationic substitution for the purpose of enhancing bioactivity. A study has recently been conducted in which titanium-substituted HA was formed for photocatalysis (Hu *et al.* 2007). As for biological coatings, some research (Lu *et al.* 2004) has been executed to develop hybrid coatings of plasma-sprayed HA and TiO₂. The goal of this work was to improve the mechanical response of the coating while attempting to further buffer the underlying alloy from releasing ions into the surrounding system. The two components remain phase separated after heat treatment. TiO₂ and HA composites formed by sol-gel have been tested for biocompatibility and cell response and results show the combination to be biocompatible and excellent at promoting cell activity (Ramires *et al.* 2001).

A range of hydroxyapatite substitutions has been investigated to date. Some substitutions such as carbonate substitutions increase the solubility of the hydroxyapatite while other substitutions, such as fluorine and chlorine decrease solubility. Overall the objective of substituting HA is to promote bone ingrowth while leaving the structure stable enough for long-term *in-vivo* application. The effects of titanium substitution are yet undiscovered.

2.3 Studying the Bioactivity of Coatings

In 1998 Larry Hench published a review of bioceramics in which he outlined the sequence of interfacial reactions which take place as tissue bonds to bioactive glass. Unfortunately there has not yet been a study which conclusively maps out the mechanism through which cell adsorption and proliferation takes place on hydroxyapatite. Many speculate as to the sequence of surface reactions which take place in the moments after an implant is placed *in-vivo*, however *in-vitro* simulations can provide some insights.

The benchmark for determining bioactivity of a bone-implant coating is whether the material promotes the crystallization of Ca-P-rich apatites once in solution. Many researchers test the rate of apatite formation on their biomaterials by conducting *in-vitro* studies using simulated body fluid (SBF). SBF is a buffered solution, created by Kokubo in the late 1980's, containing various minerals and salts present in human plasma. Researchers use techniques such as inductively coupled plasma (ICP) to quantify the changes in ion concentration in the solution. This analysis is traditionally coupled with microscopy of the coating surface to observe changes in morphology due to apatite precipitation and XRD analysis to determine crystal structure of the newly formed apatite in addition to changes in coating crystallinity. Figure 2.3 shows precipitated calcium-phosphate on the surface of HA after being immersed in SBF as well as apatite formation after 12 weeks *in-vivo* (Porter *et al.* 2004a).

(a)

QuickTime™ and a
TIFF (Uncompressed) decompressor
are needed to see this picture.

(b)

QuickTime™ and a
TIFF (Uncompressed) decompressor
are needed to see this picture.

Figure 2.3 Precipitated Ca-P on the surface of bioactive HA:

(a) Needle-like Ca-P precipitates form as the HA granule undergoes dissolution. The HA has been dispersed in simulated body fluid for 1 day.

(b) HA which was placed *in-vivo* for 12 weeks promotes the formation of bone apatite around the implant interface without dissolving.

The next step when testing the bioactivity of newly developed coatings is to observe the cell response. Many studies now use primary human cell lines, such as the osteoblast-like cells taken from the MG-63 cell line, as the standard when studying cell adsorption and proliferation. Sterilised samples are covered with cells, allowed to grow, and then fixed on the substrate for electron microscopy. Fig 2.4a shows an MG-63 cell attached to a plain titanium alloy substrate while Fig 2.4b, on the other hand, shows MG-63 cells proliferating and spreading on a bioactive surface (Kim 2004).

(a)

(b)

QuickTime™ and a
TIFF (Uncompressed) decompressor
are needed to see this picture.

QuickTime™ and a
TIFF (Uncompressed) decompressor
are needed to see this picture.

Figure 2.4 Cellular response to bioinert versus bioactive materials: (a) MG-63 cell retains spherical morphology and has not spread on the bare titanium substrate; (b) MG-63 cells have attached and proliferated on the bioactive surface. Filopodia extend from the base of the cells as they spread.

Chapter 3

Review of CaP Coating Production Methods

3.1 Introduction

While hydroxyapatite and other CaP phases find a range of applications in the human body, one area of particular interest for researchers is to develop coatings for bone implants. Figure 3.1 shows a metal implant used for hip arthroplasty including the region which is coated with HA (Jaffe and Scott 1996). There are three main categories of techniques for making hydroxyapatite coatings: plasma spraying, wet methods such as sol-gel, and physical vapour deposition, namely sputtering.

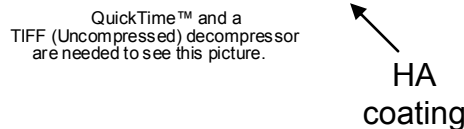


Figure 3.1 Hip-replacement prosthesis 8 years after surgery (left) and original HA-coated titanium prosthetic (right).

The common characteristics that are required of all coatings include the following: (i) good adhesion between the bioceramic and the metal implant, (ii) stable CaP phase to ensure longevity of the implant-bone fixation, (iii) uniform coating which may be used on complex shapes.

3.2 Plasma Spraying

Plasma spraying is a popular and widely-used technique to apply CaP coatings to implants. It has gained popularity over the past two decades due to its economic efficiency and scalability for large-scale production (Sun *et al.* 2001). Plasma spraying is a technique in which a feedstock, HA in a powder form, is released into a carrier gas to be transported into the plasma gun. The gun generates the plasma by maintaining a high voltage across an ionisable gas, such as argon. The powder is partially melted in the plasma (temperatures can exceed 10,000K) and is accelerated towards the substrate at which point the molten particles rapidly cool upon colliding with the substrate. Figure 3.2 shows a schematic of plasma spraying.

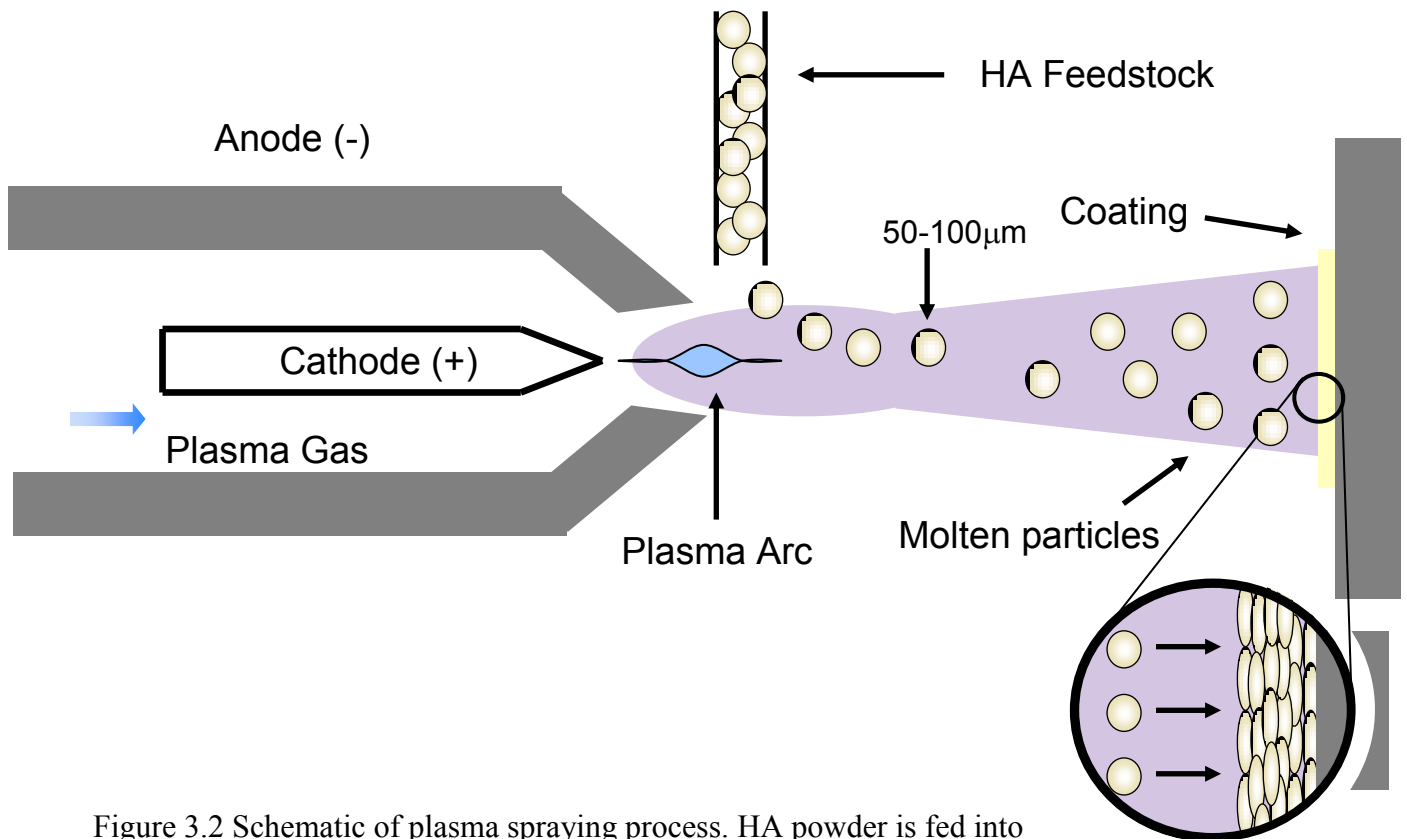


Figure 3.2 Schematic of plasma spraying process. HA powder is fed into the plasma flame. The particles arrive with both high velocity and temperature at the substrate where they stack upon one another to build up the coating.

One of the main concerns with plasma spraying is the degradation of hydroxyapatite particles into other less stable phases of CaP including tetra calcium phosphate, TCP, and amorphous CaP (Radin and Ducheyne 1992). Cao *et al.* (1996) demonstrated the effectiveness of water-vapour heat treatments to convert these phases back to crystalline HA. As a result the coating became more stable when placed in solution than as-deposited coatings. To incorporate ion

substitution into plasma-sprayed coatings, the feed powder must be substituted HA. Recent success (Xue *et al.* 2007) has been demonstrated with a plasma-sprayed strontium-substituted hydroxyapatite in which coatings with a thickness of 200-300 μm , good adhesion to the titanium alloy substrate, and improved cell response as compared to undoped HA were achieved.

During the plasma spraying process, the feedstock undergoes extreme conditions (i.e. temperatures in excess of 10,000 K). The variables which can be adjusted during plasma spraying include the size of the HA particles as well as the speed with which the particles travel towards the substrate. When the particles enter the plasma, they are accelerated towards the implant, during which time they undergo partial melting and decomposition. As a result, plasma sprayed coatings appear to include a range of crystalline HA as well as a range of CaP phases (Sun *et al.* 2001).

Achieving the optimum thickness for plasma-sprayed coatings is critical; if the coating is too thick, the shear strength is compromised making adhesion to the implant weaker. Industry manufacturers aim for coatings of 50-75 μm in thickness. (Sun *et al.* 2001). It has been demonstrated that plasma-sprayed coatings can delaminate over time which poses a problem to the longevity of bone-implant fixation. Furthermore, debris from a delaminated coating can negatively affect local bone development (Misch and Dietsh, 1993).

3.3 Sol-gel and Biomimetic Processes

Sol-gel is a method which begins with the mixing of precursors in a solvent. A heating stage is carried out to promote the formation of the desired compounds while driving off the organic components of the solvent leaving behind a coating. In the case of hydroxyapatite there are a variety of precursors that can be mixed together in an organic solvent such as ethanol. The sol is placed onto a substrate by spin or dip coating. After heating the sol and removing the solvent, the HA gel that is left over is calcined to ensure crystallinity. Typically this heat-treatment is carried out at low temperatures to prevent oxidation or phase change in a substrate.

Liu *et al.* (2001) developed sol-gel based HA using triethyl phosphite and calcium nitrate. Each precursor was hydrolyzed in water and remained in solution until heated to 60°C to

drive off the solvent. The remaining gel was then calcined at 350°C to result in a porous, crystalline layer of HA. The porous structure is believed to aid in the movement of physiological fluid through the coating in biomedical applications.

Sol-gel is an excellent coating technique for complex shapes and results in a thin coating (e.g. $< 1 \mu\text{m}$). However, the coating properties can vary greatly depending on the precursors used, the processing parameters chosen for the sol, temperature at which the films are processed, and the atmosphere in which the gel is heat-treated. Because the technique requires some heat-treatment to crystallize the coating, there is risk of oxidising the substrate. Therefore continued research in this area aims to produce crystalline coatings at the lowest temperatures possible.

A biomimetic approach to making CaP coatings relies on the natural formation of an apatite layer on a substrate once immersed in simulated body fluid (Kokubo *et al.* 2003). Simulated body fluid (SBF) is similar in composition to human blood plasma. By placing substrates in this solution at 37°C, a layer of apatite can be crystallized and grown. The process is inexpensive, simple to execute, and does not require high temperature processes or harsh chemicals. The drawback, however, is the length of time (e.g. days) needed to grow a sufficiently thick apatite layer from solution.

Lu *et al.* (2007) investigated the effects of a nitric acid treatment on titanium substrates to increase surface area for nucleation and growth of a Ca-P layer. Samples were tested in both simulated body fluid and a supersaturated calcium phosphate solution (SCPS). Results showed an amorphous layer of CaP in the SBF and an octacalcium phosphate layer in the SCPS. The CaP layer showed signs of delamination if the substrate was not of sufficient roughness. A rougher substrate increases surface area and yields better coating to substrate adhesion.

3.4 Principles of Magnetron Sputtering

The category of physical vapour deposition includes techniques such as evaporation, e-beam evaporation, pulsed laser deposition, and sputter deposition. For the purposes of this research sputtering will be looked at in closer detail. Magnetron sputtering affords a range of advantages including: (i) good adhesion and high density of films, (ii) ability to deposit metals, oxides, etc. with control over composition and stoichiometry, and (iii) high thickness uniformity and stability of deposition rate (Kukla 1997)

There are three basic components needed to make a sputtering system. The first component is a vacuum chamber. These chambers are generally made of steel and are sealed with copper gaskets for isolation from the surrounding atmosphere. The chamber is connected to a pumping system to evacuate the chamber of air and achieve an ultra-high vacuum. Once a clean vacuum is achieved, the inert sputtering gas, argon for example, is released into the chamber at a controlled rate. It is this gas which creates the plasma necessary for the sputtering to take place.

The second component of a sputtering system is a holder upon which the substrates will be placed once in the chamber. This holder is sometimes attached to an external system to control its temperature. The distance between the substrate holder and the sputtering target is a variable which must be controlled. It may be advantageous to have a rotating substrate holder to achieve uniformity.

The final component of the system is the sputtering target from which the atoms will be deposited onto the substrates. The target can be almost any material. To strike a plasma from the argon gas in the vacuum chamber the following conditions must be reached: the system must be at a low pressure (e.g. 0.5 – 5 Pa) and there must be a high negative voltage on the target (i.e. kV). The sputtering gas breakdowns into ions which are accelerated towards the target in the presence of the strong electric field.

These ions bombard the sputtering target releasing atoms or clusters of atoms. Secondary electrons, in addition to atoms, are released from the target. These electrons collide with inert gas near the target promoting a self-sustaining glow discharge. A magnet is present behind the target. The magnetic field lines penetrate the target and act to confine the electrons at the

target surface and as a result increase the rate of sputtering at the target surface. The sputtered atoms move away from the target. Some atoms are scattered while others deposit onto the substrates creating a thin film. Figure 3.3 provides a schematic of the sputtering process.

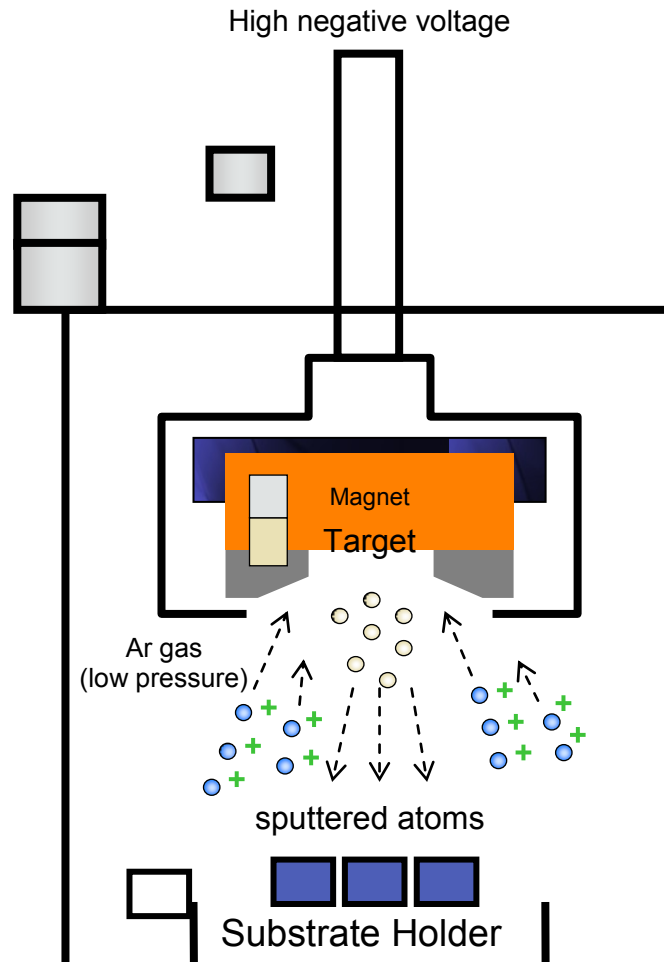


Figure 3.3 Schematic diagram illustrating magnetron sputtering system.

There are several variables during deposition which impact the rate at which the target is sputtered and material is transferred to the substrate. The primary method to control deposition rate is to adjust the power supplied to the target. Sputtering is most efficient when the mean free path of sputtered atoms is as large as possible while still maintaining a steady plasma. If the chamber pressure is increased, more ionised gas will collide with the sputtered material reducing the flux of atoms arriving at the substrate. The other variable, which can be adjusted, is the target-substrate distance. A shorter target-substrate distance will increase the rate of deposition, but at the expense of film uniformity. The substrates will also undergo heating as they are moved closer to the target.

3.5 Physicochemical Properties of Sputtered Coatings

Calcium phosphate coatings were prepared by magnetron sputtering as early as 1993 by Jansen and colleagues. In the years after the introduction of this deposition method, much research has been done to manipulate deposition conditions and heat treatments to optimize the coating properties.

Sputtered coatings of calcium-phosphate have shown higher than expected Ca/P ratios. Ozeki and colleagues (2002) prepared coatings sputtered from a stoichiometric hydroxyapatite target with calcium-phosphate (Ca/P) ratio of 1.67 (prepared by wet precipitation and crystallized at 900°C). The target-substrate distance was 60mm. The deposition pressure was varied from 0.5 to 5 Pa and target power density varied from 2.54 to 7.64 W cm⁻¹. Ca/P ratios (obtained by energy-dispersive x-ray spectroscopy, EDS) as high as 2.43 ± 0.07 were observed, values significantly higher than that of the stoichiometric target.

van Dijk (1996) prepared 2 µm thick samples of sputtered calcium phosphate from a plasma-sprayed target. Rutherford backscattered spectrometry (RBS) was used to obtain the Ca/P ratio. As deposited samples had a Ca/P ratio of 2.1 as compared to the stoichiometric 1.67 for HA. Heat treatments reduced the Ca/P ratio, however the stoichiometric value could not be obtained.

To counter the higher Ca/P ratio from sputtered hydroxyapatite van Dijk *et al.* (1997) took a different approach. van Dijk and colleagues prepared thin coatings of sputtered Ca₅(PO₄)₃OH using a plasma-sprayed target. Ti6Al4V discs were used as substrates and the target-substrate distance was set at 75 mm. The deposition variables included pressure (0.3 and 1.5 Pa) and power level. Sputtering time was 2 hours and oxygen was added to the sputtering chamber at 5, 10, and 50% of the argon pressure. The additional oxygen reduced the deposition rate and also suppressed the preferential re-sputtering of phosphorous from the film thus bringing the Ca/P ratio to the stoichiometric 1.67 desired of HA coatings.

More recently Boyd *et al.* (2007) produced a range of magnetron sputtered calcium-phosphate samples with a range of Ca/P ratios by adjusting the pressure of the argon sputtering gas during deposition. The objective of this study was to use multiple HA targets during deposition combined with different pressures to achieve a variety of Ca/P coatings.

The samples were heat-treated to 500°C for two hours. The composition of films was determined using x-ray photoelectron spectroscopy (XPS), a technique which is not traditionally used to obtain the Ca/P ratio, which gave Ca/P ratios for heat-treated samples ranging from 3.38 ± 0.11 (1 Pa) to 1.82 ± 0.06 (5 Pa). The stoichiometric Ca/P ratio of HA is 1.67 as presented in Table 2.1.

3.5.1 Heat treatment of Sputtered Coatings

The post-deposition heat treatment of sputtered films is critical to achieve a crystalline film. van Dijk and colleagues (1996) investigated the effects of different heat treatments on sputtered calcium phosphate coatings. 2 µm thick samples were formed by sputtering. Samples were heat treated under an argon and argon-water vapour atmosphere at temperatures of 400, 600, 800, 1000, and 1200°C. Results showed the samples formed crystalline HA at 600°C in both argon and argon-water vapour atmospheres.

More recently Yang *et al.* (2003) conducted a similar investigation on the crystallinity of calcium phosphate coatings as a function of temperature and the presence of water vapour. Using XRD they found a difference in the degree of crystallinity, 68% as opposed to 2%, when water vapour is present at 450°C. At temperatures above 450°C it was concluded that the presence of water vapour did not have a significant effect on crystallinity.

3.5.2 *In-vivo* Study of Sputtered Coatings

Wolke *et al.* (1997) prepared sputtered Ca-P coatings on pure titanium discs using a plasma-sprayed target. Coatings at thicknesses of 0.1, 1, and 4 µm were sputtered with an r.f. power source. Half of the samples were heat treated at 500°C for 2 hours. The discs were prepared so they could be implanted into rabbits to study the *in-vivo* dissolution of the coatings. It was discovered that as-deposited coatings dissolved too rapidly. Heat-treated samples dissolved at an optimal rate *in-vivo* and showed signs of apatite growth on the coating during the study.

3.5.3 Sputtering of Doped-Hydroxyapatite Thin Films

The importance of substitutions into HA (Section 2.2.2) have been presented in addition to various techniques to make implant coatings. Traditional methods for forming doped hydroxyapatite have focused on wet precipitation. Recently, substituted or doped hydroxyapatite coatings have been developed through magnetron sputtering (Chen *et al.* 2006, Porter *et al.* 2004b, Thian *et al.* 2005, 2006). There are two ways in which a substituted hydroxyapatite could be sputtered. One method would be to fabricate a doped target from which the coating could be deposited. This route would be intensive and would restrict the composition of doped films. The more popularly adopted alternative is magnetron co-sputtering.

Porter *et al.* (2004b) developed the first silicon-substituted hydroxyapatite thin films using magnetron co-sputtering. Thin films (100 to 150 nm) were fabricated by depositing at a rate of 0.85 nm/min at a pressure of 0.85 Pa. The phase-pure HA target was slip-cast and sintered and the commercial Si target was 99.999% pure.

This work was then advanced by Thian *et al.* (2005) in which films of 600 nm doped with 0.8 wt.% Si were formed by co-sputtering. As-deposited films were heat-treated for 3 hours in a 700°C argon-water vapour atmosphere. Crystalline films, confirmed by XRD, were then placed *in-vitro* with human osteoblast-like cells. These cells showed optimal response on heat-treated Si-substituted HA films. Thian *et al.* (2006) extended their work to make coatings with 0.8, 2.2 and 4.9 wt. % silicon. Osteoblast attachment, proliferation, and differentiation during this long-term *in-vitro* study showed great promise for these co-sputtered coatings to be used *in-vivo*.

Chen and colleagues (2006) developed functionalized hydroxyapatite coatings by investigating the antibacterial properties of silver when added to HA. To address the issue of bacterial infection after implant procedures, a co-sputtered coating of hydroxyapatite and silver was created. After a 3 hour deposition of Ag (10W) and HA (300W) a 4 hour heat treatment at 400° C created crystalline HA with phase separated silver. The doped coating appeared to inhibit the growth of bacteria *in-vitro*. No cytotoxicity of the coatings was observed.

3.6 Summary

While many techniques may be used to develop Ca/P coatings for use in biomedical implants, magnetron co-sputtering provides the opportunity to easily develop a range of doped hydroxyapatite coatings. A wide range of characterization methods have been applied to the study of HA. Profilometry and EDS are commonly used methods for determining the thickness and composition of Ca/P coatings. Fourier-transform Infrared Spectroscopy (FTIR) provides detailed information on the molecular structure of HA, but requires operation in glancing-angle or reflection mode for thin films. Raman spectroscopy has not been used extensively with HA, but provides similar information to FTIR regarding molecular structure. XPS provides analysis of the surface chemistry of coatings and can provide insight into the bonding state of atoms present. XRD has become a commonly accepted method for investigating the crystallinity of HA.

It was the intention of this project to use the versatility of magnetron co-sputtering to investigate the effects on hydroxyapatite when doped with a small amount of titanium. A range of characterization techniques (profilometry, EDS, XRD, XPS, Raman Spectroscopy) will elucidate some of the materials properties of HA-Ti coatings. Preliminary human osteoblast cell response to HA-Ti coatings will be observed *in-vitro*.

Chapter 4

Experimental Methods for Film Fabrication

4.1 Substrates & Targets

Polished single crystal (100) silicon was manually cleaved using a diamond scribe into squares approximately 1cm by 1cm to be used as substrates. Silicon (Si) was selected as the substrate material because it is easy to cleave and it is stable at high temperatures. Silicon substrates also have a smooth, polished surface meaning a step height can be easily measured when determining film thickness. Should work be carried out to determine the release rate of titanium atoms from the hydroxyapatite films, the substrate cannot be made of titanium.

Substrates were cleaned in an ultrasonic acetone bath for 3 minutes and dried with compressed air. Approximately 20-25 substrates were positioned together on the substrate holder during each deposition. A titanium (Ti, 99.6% pure) target along with a homemade hydroxyapatite (HA) target were used as sputtering targets with dimensions of 55mm by 35 mm.

The HA target was slip-cast from a slurry of precipitated HA and sintered to form a dense, single-phase target. (prepared by Junyi Ma, Cambridge Centre for Medical Materials). The precipitated HA powder was dried and calcined. The calcined powder was then suspended in deionised water and polymer dispersant before undergoing a 3-day ball milling process. The slurry was then poured onto a plaster plate within a mold. After adequate drying, the target was sintered (120°C for 4 hours to eliminate water in samples followed by 1200°C for 2 hours). The sample was polished down to dimensions of 55mm by 35mm by 2-3mm, cleaned in acetone, and oven dried. The target was characterized with XRD and EDS which showed a phase-pure HA target with a Ca/P ratio of approximately 1.67.

4.2 Magnetron Co-sputtering

HA-Ti coatings were prepared using a customized deposition system with two targets. Both the HA and Ti targets were affixed to water-cooled magnetrons with a separation distance of 105mm. The Si substrates were placed on a flat substrate-holder 44mm below the targets. The chamber was evacuated using a rotary roughing pump followed by a turbo-molecular

pump bringing the base pressure to 1×10^{-7} Pa after an overnight pump. The deposition was carried out at room temperature while a continuous flow of high-purity argon (Ar) gas was delivered into the sputtering chamber maintaining the working pressure at 0.8 Pa. The sputtering time for all depositions was 6 hours.

The radio-frequency power (13.56 MHz) supplied to the HA target was limited to 60 W (3.11 W cm^{-2}). At higher power the ceramic target was likely to heat and crack. The deposition rate from this ceramic target was very low in comparison to the metallic Ti target. To achieve various concentrations of Ti in the thin films, the direct-current power to the Ti target was supplied at 5, 10 and 15 W. The power supply used for direct-current (dc) sputtering was unstable when supplying power below 5W and would have prevented reproducible results.

Both targets were pre-sputtered while a rotatable shutter shielded the substrates. Pre-sputtering took place for approximately 10 minutes prior to starting the deposition to remove any adsorbed contaminants from the surface of the targets and to allow the deposition parameters to be set (i.e. pressure and power). Co-sputtering of both the HA and Ti targets at equal rates would result in Ti concentrations beyond the desired amount. To reduce the rate of Ti deposition, a shutter with holes was placed in front of the Ti target during deposition to reduce the flux of Ti atoms arriving at the substrates. The substrates were also placed in front of the HA target to reduce the flux of titanium even further. A composition gradient was avoided by placing all substrates within a narrow region beneath the HA target. Figure 4.1 presents a schematic of the deposition chamber.

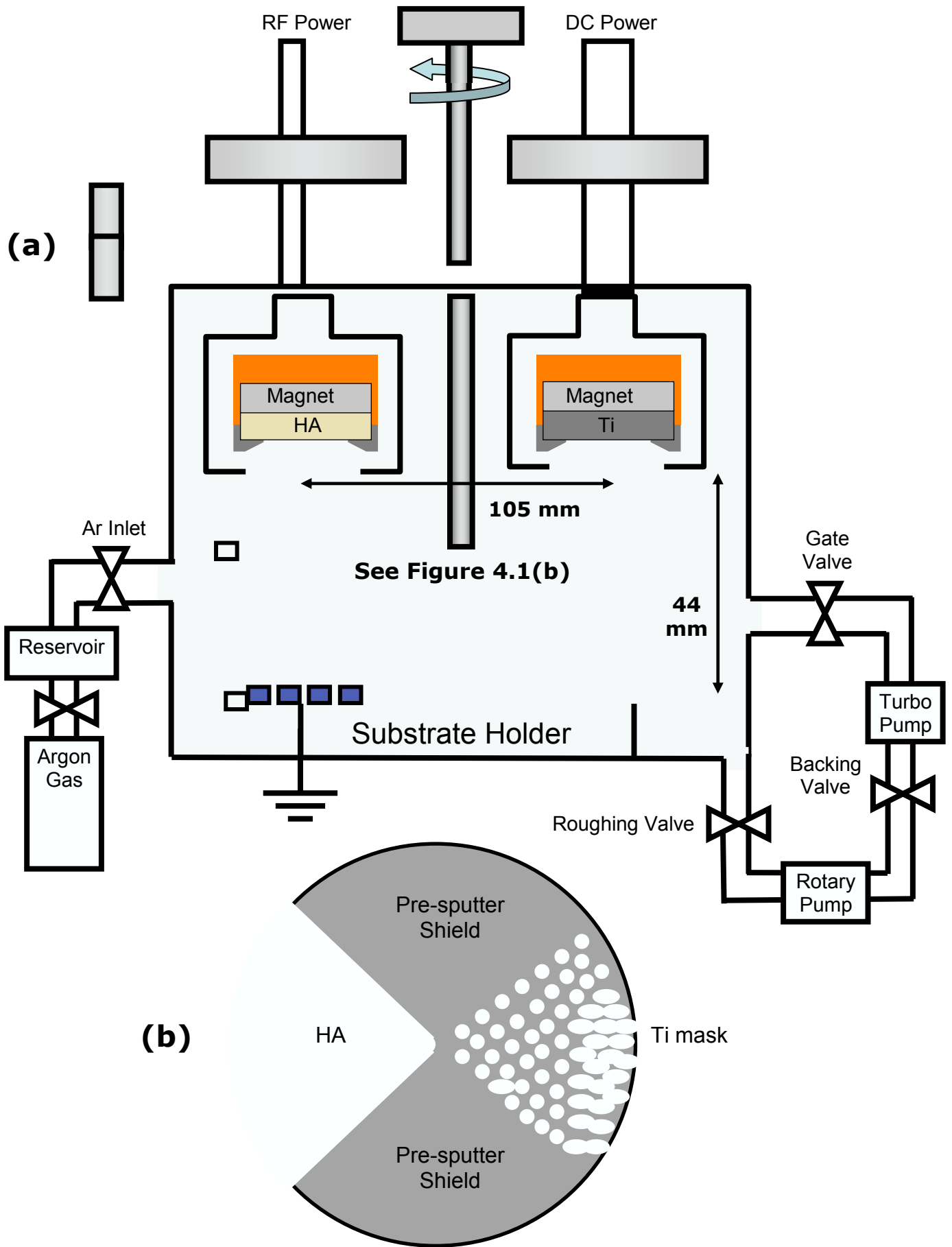


Figure 4.1 (a) Schematic diagram of co-sputtering system, (b) schematic of rotatable shield/mask

4.3 Heat Treatment

As-deposited samples underwent two different heat treatments in tube furnaces. Samples were heated at a rate of 2.5 °C/min to a temperature of 700 °C and maintained for 4hrs. The furnace atmosphere was either an argon gas or a water vapour-argon mixture (Ar + H₂O). The water-vapour was introduced into the sealed tube-furnace by bubbling argon through a flask of deionised water before it entered the furnace. Table 4.1 outlines the atmosphere and deposition conditions for various samples.

Table 4.1 Crystallization atmosphere and sputtering conditions for HA-Ti films.

Sample	Ti-power (W)	Atmosphere
A1	5	Ar
A2	10	Ar
A3	15	Ar
B1	5	Ar + H ₂ O
B2	10	Ar + H ₂ O
B3	15	Ar + H ₂ O

Ti-power: direct-current power to Ti target

Temperature: 700°C for all samples

Heat treatment dwell time = 4hrs

Radio-frequency power to HA target = 60W

For XPS analysis (Section 5.4) a sample was heated to 500°C for 2hrs in an argon-water vapour atmosphere.

References

- Barralet J, Best S, and W. Bonfield, Carbonate substitution in precipitated hydroxyapatite: an investigation into the effects of reaction temperature and bicarbonate ion concentration, *J. Biomed. Mater. Res.* **41**. 1998.
- Boyd AR, Duffy H, McCann R, *et al.* The Influence of argon gas pressure on co-sputtered calcium phosphate thin films. *Nucl. Instrum. Methods Phys. Res., Sect. B.* **258** (2):421-428. 2007.
- Brown WE, Smith JP, Lehr JR and Frazier AW. Crystallographic and chemical relations between octacalcium phosphate and hydroxyapatite, *Nature* **196**: 1050–1055. 1962.
- Cao Y, Weng J, Chen JY, *et al.* Water vapour-treated hydroxyapatite coatings after plasma spraying and their characteristics. *Biomater.* **17** (4): 419-424. 1996.
- Cao N, Ma QS, Sui JL, *et al.* The experiment of plasma-sprayed HA coatings on carbon/carbon composites in bone. *Surf. Rev. Lett.* **13** (4): 423-428. 2006.
- Carlisle EM. Silicon; a possible factor in bone calcification. *Science* **167**: 279-280. 1970.
- Carlisle EM. Silicon: an essential element for the chick. *Science* **78**: 619-621. 1972.
- Carlisle EM. A skeletal alteration associated with silicon deficiency. *Fed. Proc.* **32**: 930. 1973.
- Carlisle EM. Biochemical and morphological changes associated with long bone abnormalities in silicon deficiency. *J. Nutr.* **110**: 1046-1055. 1980.
- Chen W, Liu Y, Courtney HS, *et al.* In vitro anti-bacterial and biological properties of magnetron co-sputtered silver-containing hydroxyapatite coating. *Biomater.* **27** (32): 5512-5517. 2006.
- Dorozhkin SV. Calcium orthophosphates. *J. Mater. Sci.* **42**: 1061-1095. 2007.
- Driessens FCM, Verbeeck RMH, Kiekens P. Mechanism of substitution in carbonated apatites. *Z. Anorg. Allg. Chem.* **504** (9): 195-200. 1983.
- Fernandez E, Gil FJ, Ginebra MP, *et al.* Calcium phosphate bone cements for clinical applications - Part I: Solution chemistry. *J. Mater. Sci. - Mater. Med.* **10** (3): 169-176. 1999.
- Fleet ME, Liu X. Coupled substitution of type A and B carbonate in sodium-bearing apatite. *Biomater.* **28** (6): 916-926. 2007.
- Froimson MI, Garino J, Machenaud A, *et al.* Minimum 10-year results of a tapered, titanium, hydroxyapatite-coated hip stem. *Journal of Arthroplasty.* **22** (1): 1-7. 2007.

- Gibson IR, Akao M, Best SM and Bonfield W. Phase transformations of tricalcium phosphates using high temperature x-ray diffraction. In: Bioceramics, Proceedings of the 9th international Symposium on Ceramics in Medicine. Eds. Kokubo T, Nakamura T, Fumiaki M. pp.173-176. 1996.
- Gibson IR, Best SM and Bonfield W. Chemical characterization of silicon-substituted hydroxyapatite. *J. Biomed. Mater. Res.* **44** (4): 422-428. 1999.
- Gibson IR and Bonfield W, Preparation and characterization of magnesium/carbonate co-substituted hydroxyapatites, *J. Mater. Sci. - Mater. Med.* **13**: 685-693. 2002.
- Hu AM, Li M, Chang CK, et al. Preparation and characterization of a titanium-substituted hydroxyapatite photocatalyst. *J. Mol. Catal. A: Chem.* **267** (1-2): 79-85. 2007.
- Ihara H, Kumashiro Y, Itoh A, Maeda K. *Jpn. J. Appl. Phys.* **12**: 1462. 1973.
- Ilich JZ, Kerstetter JE. Nutrition in bone health revisited: A story beyond calcium. *J. American College of Nutrition.* **19** (6): 715-737. 2000.
- Jaffe WL, and Scott DF. Current Concepts Review - Total Hip Arthroplasty with Hydroxyapatite-Coated Prostheses. *J. Bone and Joint Surgery* **78**: 1918-34. 1996.
- Kakei M, Nakahara H, Tamura N, et al. Behavior of carbonate and magnesium ions in the initial crystallites at the early developmental stages of the rat calvaria. *Annals of Anatomy – Anatomischer Anzeiger.* **179** (4): 311-316. 1997.
- Kannan S, Ventura JM and Ferreir JMF. Aqueous precipitation method for the formation of Mg-stabilized β -tricalcium phosphate: An X-ray diffraction study. *Ceram. Int.* **33** (4): 637-641. 2007.
- Kay MI, Young RA and Posner AS. Crystal Structure of Hydroxyapatite. *Nature* **204**: 1050-1052. 1964.
- Kim HK, Jang JW, Lee CH. Surface modification of implant materials and its effect on attachment and proliferation of bone cells. *J. Mater. Sci. - Mater. Med* **15** (7): 825-830. 2004.
- Kim SR, Lee JH, Kim YT, et al. Synthesis of Si, Mg substituted hydroxyapatites and their sintering behaviours. *Biomater.* **24** (8): 1389-1398. 2003.
- Kitsugi T, Nakamura T, Oka M, Yan WQ, Goto T, Shibuya T, Kokubo T and Miyaji S. Bone bonding behavior of titanium and its alloys when coated with titanium oxide (TiO₂) and titanium silicate (Ti₅Si₃). *J. Biomed. Mater. Res.* **32** (2): 149-156. 1996.
- Kokubo T, Hayashi T, Sakka S, et al. Bonding between bioactive glasses, glass-ceramics or ceramics in a simulated body-fluid. *Yogyo-Kyokai-Shi.* **95** (8): 785-791. 1987.
- Kokubo T, Kim HM, Kawashita M. Novel bioactive materials with difference mechanical properties. *Biomater.* **24**, 2003.

- Kukla, R. Magnetron sputtering of large scale substrates: an overview on the state of the art. *Surf. Coat. Technol.* **93**. 1997.
- Landi E, Tampieria A, Mattioli-Belmonteb M, et al. Biomimetic Mg- and Mg,CO₃-substituted hydroxyapatites: synthesis characterization and in vitro behaviour. *J. Eur. Ceram. Soc.* **26** (13): 2593-2601. 2006.
- Landi, E. Biomimetic Mg-substituted hydroxyapatite: from synthesis to in vivo behaviour. *J. Mater. Sci. - Mater. Med.* 2007.
- Landis WJ, Martin JR. X-ray photoelectron-spectroscopy applied to gold-decorated mineral standards of biological interest. *J. Vac. Sci. Technol., A.* **2** (2): 1108-1111. 1984.
- Landis WJ, Lee DD, Brenna JT, Chandra S and Morrison GH. Detection and localisation of silicon and associated elements in vertebrate bone tissue by imaging ion microscopy. *Calcif. Tiss. Int.* **38**: 52-59. 1986.
- Li P, De Groot K and Kokubo T, Bioactive Ca₁₀(PO₄)₆(OH)₂-TiO₂ composite coating prepared by sol-gel process. *J. Sol-Gel. Sci. Technol.* **7**: 27-34. 1996.
- Lin FH, Liao CJ, Chen KS, Sun JS and Lin CP. Petal-like apatite formed on the surface of tricalcium phosphate ceramic after soaking in distilled water. *Biomater.* **22**: 2981. 2001.
- Liu DM, Troczynski T, Tseng WJ. Water-based sol-gel synthesis of hydroxyapatite: process development. *Biomater.* **22** (13): 1721-1730. 2001.
- Lu X, Zhao ZF, Leng Y. Biomimetic calcium phosphate coatings on nitric-acid-treated titanium surfaces *Mater. Sci. Eng., C.* **27** (4): 700-708. 2007.
- Lu YP, Li MS, Li ST, et al. Plasma-sprayed hydroxyapatite plus titania composite bond coat for hydroxyapatite coating on titanium substrate. *Biomater.* **25** (18): 4393-4403. 2004.
- Misch CE, Dietsch F. Bone-grafting materials in implant dentistry. *Implant Dent.* **2**: 158-167. 1993.
- Ozeki K, Yuhta T, Fukui Y, et al. Phase composition of sputtered films from a hydroxyapatite target. *Surf. Coat. Technol.* **160** (1): 54-61. 2002.
- Patel N, Best SM, Bonfield W, Gibson IR, Hing KA, Damien E. and Revell PA. A comparative study on the in vivo behavior of hydroxyapatite and silicon substituted hydroxyapatite granules. *J. Mater. Sci. - Mater. Med.* **13** (12). 2002.
- Porter AE, Patel N, Skepper JN, Best SM and Bonfield W. Comparison of in vivo dissolution processes in hydroxyapatite and silicon-substituted hydroxyapatite bioceramics. *Biomater.* **24**. 2003.

- Porter AE, Botelho CM, Lopes MA, Santos JD, Best SM and Bonfield W. Ultrastructural comparison of dissolution and apatite precipitation on hydroxyapatite and silicon-substituted hydroxyapatite in vitro and in vivo. *J. Biomed. Mater. Res., Part A*. **69A** (4): 670-679. 2004a.
- Porter AE, Rea SM, Galtrey M, et al. Production of thin film silicon-doped hydroxyapatite via sputter deposition. *J. Mater. Sci.* **39** (5): 1895-1898. 2004b.
- Radin SR and Ducheyne P. Plasma spraying induced changes of calcium-phosphate ceramic characteristics and the effect on *in vitro* stability. *J. Mater. Sci. - Mater. Med.* **3** (1): 33-42. 1992
- Ramires PA, Romito A, Cosentino F, et al. The influence of titania/hydroxyapatite composite coatings on in vitro osteoblasts behaviour. *Biomater.* **22** (12): 1467-1474. 2001.
- Roemhildt, M. L. Characterization of a novel calcium phosphate composite bone cement: Flow, setting, and aging properties. *J. Mater. Sci. - Mater. Med.* **17** (11), 2006.
- Romo LA. Synthesis of Carbonate-apatite. *J. Am. Chem. Soc.* **76** (15): 3924-3925. 1954.
- Serre CM, Papillard M, Chavassieux P, Voegel JC and Boivin G. Influence of magnesium substitution on a collagen-apatite biomaterial on the production of a calcifying matrix by human osteoblasts. *J. Biomed. Mater. Res.* **42** (4): 626-633. 1998.
- Shi, Donglu. Introduction to Biomaterials. Tsinghua University Press. 2006.
- Skrtic D, Antonucci JM, Eanes ED, et al. Dental composites based on hybrid and surface-modified amorphous calcium phosphates. *Biomater.* **25** (7-8): 1141-1150. 2004.
- Song YX, Feng ZD and Wang T. In situ study on the curing process of calcium phosphate bone cement. *J. Mater. Sci. - Mater. Med.* **18** (6): 1185-1193. 2007.
- Sun L, Berndt CC, Gross KA and Kucuk A. Material Fundamentals and Clinical Performance of Plasma-Sprayed Hydroxyapatite Coatings: A Review. *J. Biomed. Mater. Res. (Appl. Biomater.)* **58**. 2001.
- Suzuki O, Kamakura S, Katagiri T, et al. Bone formation enhanced by implanted octacalcium phosphate involving conversion into Ca-deficient hydroxyapatite. *Biomater.* **27** (13): 2671-2681. 2006.
- Tadic D., Peters F., Epple M., Continuous synthesis of amorphous carbonated apatites. *Biomater.* **23**: 2553-2559. 2002.
- Takagi S, Chow LC and Ishikawa K. Formation of hydroxyapatite in new calcium phosphate cements. *Biomater.* **19** (17): 1593-1599. 1998.
- Thian ES, Huang J, Best SM, et al. Magnetron co-sputtered silicon-containing hydroxyapatite thin films - an in vitro study. *Biomater.* **26** (16): 2947-2956. 2005.

- Thian ES, Huang J, Vickers ME, et al. Silicon-substituted hydroxyapatite (SiHA): A novel calcium phosphate coating for biomedical applications. *J. Mater. Sci.* **41** (3): 709-717. 2006.
- Van Dijk K, Schaeken HG, Wolke JGC, et al. Influence of annealing temperature on RF magnetron sputtered calcium phosphate coatings. *Biomater.* **17** (4): 405-410. 1996.
- Van Dijk K, Verhoeven J, Maree CHM, et al. Study of the influence of oxygen on the composition of thin films obtained by r.f. sputtering from $\text{Ca}_5(\text{PO}_4)_3\text{OH}$ target. *Thin Solid Films* **304**: 191-195. 1997.
- Wen HB, de Wijn JR, Cui FZ, et al. Preparation of bioactive Ti6Al4V surfaces by a simple method. *Biomater.* **19** (1-3): 215-221. 1998.
- Wolke JGC, de Groot K and Jansen JA. In vivo dissolution behavior of various RF magnetron sputtered Ca-P coatings. *J. Biomed. Mater. Res.* **39**: 524-530. 1997.
- Wong M, Eulenberger J, Schenk R and Hunziker E. Effect of surface topology on the osseointegration of implant materials in trabecular bone. *J. Biomed. Mater. Res.* **29** (12): 1567-1575. 1995.
- Wu CT and Chang J. Bonelike apatite formation on carbon microspheres. *Mater. Lett.* **61** (11-12): 2502-2505. 2007.
- Xue WC, Hosick HL, Bandyopadhyay A, et al. Preparation and cell-materials interactions of plasma sprayed strontium-containing hydroxyapatite coating. *Surf. Coat. Technol.* **201** (8): 4685-4693. 2007.
- Yang Y, Kim KH, Agrawal CM and Ong JL. Effect of post-deposition heating temperature and the presence of water vapour during heat treatment on crystallinity of calcium phosphate coatings. *Biomater.* **24**: 5131-5137. 2003.